Energetic Optimization of an Automotive Paintshop Using Dynamic Thermo-Fluid Simulation

A. Phong Tran*
German Aerospace Center (DLR)
Institute of Low-Carbon Industrial Processes
e–mail: Anh.Tran@dlr.de

Johannes-Jarik Siegel, Jasper Walden, Adrian Bamler

ABSTRACT

The vehicle painting process is typically the most energy-intensive process within an automotive manufacturing plant. Meeting the temperature and humidity requirements during the painting application and drying stages necessitates significant energy consumption for heating and cooling in paintshops. The energy consumption of a paintshop is dynamic and heavily influenced by external factors such as weather conditions and production schedules. Consequently, it becomes a challenging task to accurately assess the energetic impact of plant modifications. This study focuses on optimizing an automotive paintshop through the application of a validated dynamic model of the facility. The dynamic model is implemented using Modelica and captures main painting processes such as pre-treatment, drying ovens and HVAC units. The model is calibrated using transient data collected from the actual plant. A wide range of energy optimization strategies is presented, encompassing improvements in heat recovery, airflow management, and control systems. The energy saving potential of each measure is estimated using the dynamic model by simulating the model for one typical year. The results indicate that these measures can reduce energy demand significantly: A shift to a three-shift schedule lowers energy demand per vehicle by 10.4%. Integrating a heat pump into pre-treatment and e-coat processes achieves a combined COP of 5.12. Additionally, optimizing an air supply unit's controller decreases its annual energy demand by 46.5%.

KEYWORDS

Dynamic simulation, Modelica, automotive paintshop, thermofluid simulation, HVAC

INTRODUCTION

The production of cars involves a series of energy-intensive processes. According to manufacturers, each vehicle requires approximately 2 MWh of energy [1, 2]. A large share of the energy is required in the paintshop which consumes more than a third of the total consumption, as reported by Giampieri et al. [3]. Although there are efforts to reduce the carbon footprint of the paintshop's heating demand, most plants still rely on gas-fired heating. Automotive manufacturers have pledged to achieve net-zero carbon production of their cars. To further this goal, researchers have developed methods to improve the understanding of paintshop processes and conducted studies on enhancing energy efficiency. For this purpose, researchers have developed methods to further the understanding of paintshop processes and conducted studies on improving energy efficiency. Of particular interest is the optimization of

* Corresponding author

air conditioning in paintshops. Giampieri [4] investigates liquid dessicant technology to improve air conditioning, and Alt [5] proposes a method to synthesize a controller for paint booth air supply units. Wendt [6] presents a holistic method for assessing energy efficiency of optimization measures using a paintshop model composed of subprocess models. Furthermore, researchers have identified the drying ovens as a potential focal point for optimization due to the high temperatures involved: Johnson [7] developed a high-fidelity heat transfer model of a paintshop's convective drying oven. Daniarta [8] researches the waste heat recovery potential through organic Rankine cycles and thermal energy storages in paintshops.

The present study approaches the challenge in a similar manner to Giampieri [9], where thermodynamic models of painting processes are used to assess the impacts of sustainable technologies on energy demand while considering annual weather fluctuations. In this study, we propose a methodology for assessing the effects of technical modifications or optimization measures on a plant's energy efficiency using dynamic models of paintshop processes. The models are based on first-principle thermo and fluid dynamic conservation laws and are calibrated using transient measurement data from an operating automotive paintshop. The calibrated models allow for the implementation of larger models of various parts of the plant, ranging from single air supply unit models to entire paintshops. This study presents a whole-year simulation of a paintshop and analyzes three different optimization measures.

DYNAMIC MODELLING OF AN AUTOMOTIVE PAINTSHOP

Modern automotive coatings consist of multiple layers of paint applied to the body by either e-coating (also known as cathodic electrodeposition or CED) or spraying. The paintshop system investigated in this study is a typical automotive paintshop, as shown in Figure 1. The multi-layer structure of the car coating is reflected in the paintshop process: after each layer of paint is applied, the car undergoes a drying process before the next layer is added. Processes in the paintshop, such as drying ovens or air supply units, are often similar in structure and only differ in size. For this reason, reusable models have been implemented using the modelling language Modelica. The models are based on existing models taken from the Buildings library [10] and the Modelica Standard Library.

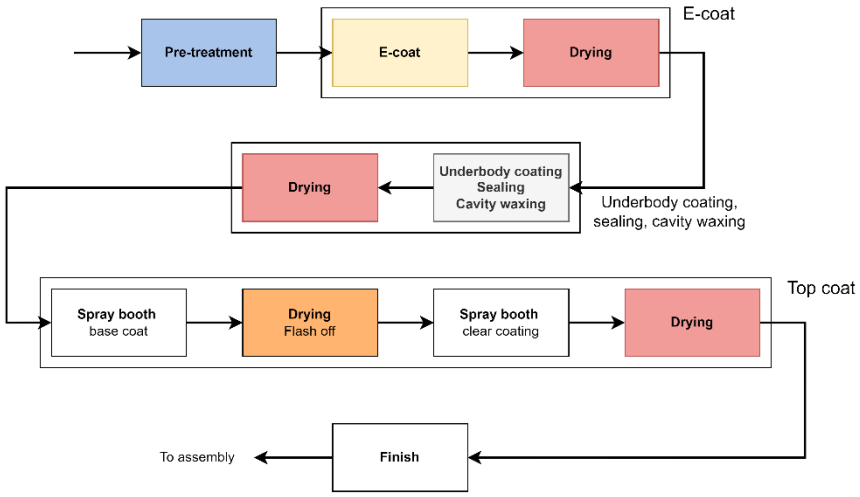

Figure 1: A simplified schematic of the investigated paintshop, adapted from [11] and [3]

The aim of this study is to implement a dynamic model of the automotive paintshop capable of reproducing and predicting energy consumption. The following sections provide insight into the modelling of paintshop processes.

Pre-treatment and e-coating

The pre-treatment process consists of several immersion tanks in which the cars are washed, phosphated and rinsed. To model the large volumes of water (up to 250 m³) used in the tanks, ideal mixing volume models are utilized, considering various heat loss mechanisms such as heat absorption by the cars, convective heat losses, and cooling via sprayed water. The model uses a surrogate equation with empirical coefficients to model the load-dependent fractions of the heat loss. Convective heat loss, which is largely independent of load, is depicted by a constant thermal resistance between the tank water and the surrounding air. Furthermore, a heat capacitor that models the housing's heat capacity is connected to the water volume.
The pre-treatment and e-coating tanks are equipped with water recirculation pumps that deliver constant mass flow rates at nominal pressure heads, adding heat to the circulated water. Some tanks use a heat exchanger to control water temperature by heating or cooling circulated water with a refrigerant. The refrigerant pump operates at a constant mass flow rate in a mixing circuit.

Heating, ventilation and air conditioning (HVAC)

The paintshop employs numerous HVAC units in different configurations and sizings. To capture these configurations, a reusable HVAC template was implemented. The template is shown in Figure 2 and enables HVAC models consisting of up to four components.

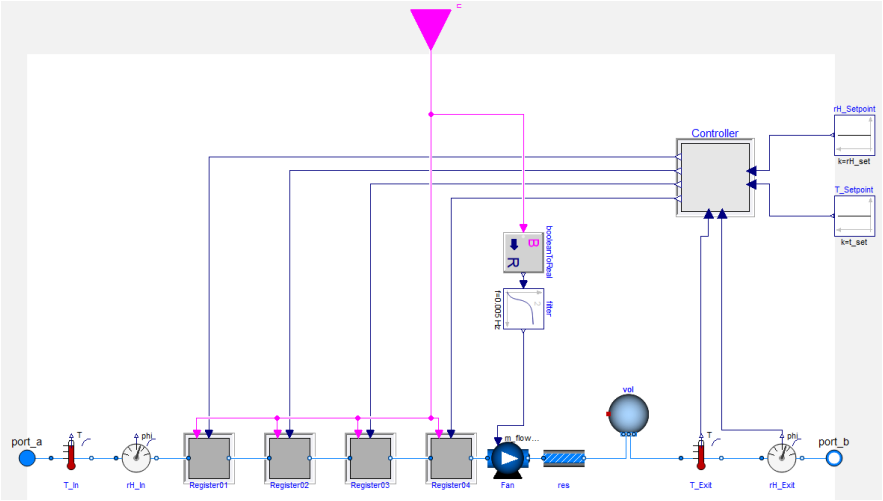

Figure 2: HVAC template model used to model almost all HVAC systems in the plant

Each of the four components can be replaced by the user with one of the following models:

- Direct heater: Air is directly heated by burning gas (e.g. line burners).
- Heat exchanger: Air is heated with a heat transfer medium via a heat exchanger. The heat transfer medium is flowing in a mixing circuit and is controlled using a three-way valve.
- Cooler/dehumidifier: Air is cooled with a refrigerant in a heat exchanger. A discretized heat exchanger model is used to calculate the metal temperatures and as a result, the mass flow rate of the condensing water.
- Spray humidifier: Water is added to the air flow in a near-isenthalpic change of state.

Every HVAC unit is equipped with a fan that is modeled using nominal values for mass flow rate and pressure rise. A constant hydraulic effectiveness and quadratic flow characteristic is assumed. The HVAC components are modeled with two input signals: A continuous signal can be varied to manipulate the internal actuator (e.g. valve opening, added water or added heat

flow rate). A boolean (on/off) signal can be set to turn the component off. This is required to differentiate between operation at minimum load and when the system is switched off entirely (e.g. for gas burners).

Additionally, a controller needs to be defined to manipulate the components' input variables. The controller shown in Figure 2 is replaceable and is provided with measurements of temperature and relative humidity. Each configuration requires the implementation of a specialized control scheme that generates the actuator signals.

Drying ovens

The paintshop uses multi-zone drying ovens to dry car bodies after applying a layer of paint. The temperature of these ovens ranges from 90 to 200°C, depending on the paint composition. After drying, the car bodies are moved to cooling zones to cool down before proceeding to the next production stage.

During the drying process, volatile organic compounds (VOCs) are released into the drying air. The polluted air from all drying ovens is collected and routed to a thermal oxidizer, where the VOCs are removed via a direct-fired thermal oxidizer (DFTO) or a regenerative thermal oxidizer (RTO). The model considers the addition of VOCs to the dryer air based on exhaust gas analysis results. The heating value of the VOCs contributes to the heating in the DFTO and RTO.

Reusable models for the drying zones, cooling zones and thermal oxidizers are implemented and connected to a drying oven model. The drying zone model accounts for heat losses, including car heat absorption and convective heat to ambient air, using a lumped heat capacitor for housing material heat capacity.

A fan draws air from the oven to a heater box, where it's heated and recirculated. Depending on the type of thermal oxidizer, air is heated either by the exhaust gases through a heat exchanger or by gas burners. A controller adjusts the valve or burner to maintain the set-point temperature of the hot air supply.

MODEL CALIBRATION

The model includes parameters that are typically challenging to determine and are not included in the process diagram or manufacturer datasheet, such as efficiencies, pressure losses, or heat losses. To calibrate these parameters, measured data from the plant is used. All modeled processes were calibrated with available data. This section presents a selection of the calibration results to illustrate the calibration process.

Air supply units with heat recovery

This section presents the calibration of a paint booth air supply unit depicted in Figure 3. Air from outside is drawn through a thermal wheel, thereby recovering heat and moisture from the exhaust air flow. The air supply unit uses a cooling, heating and humidification to condition the air to the required temperature and humidity.

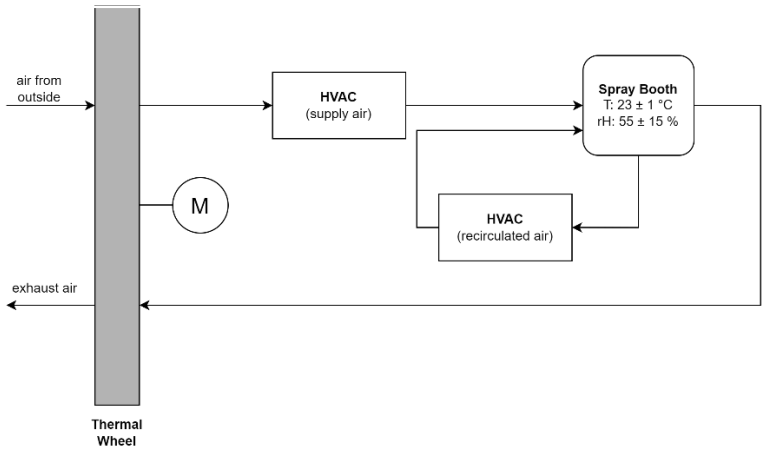

Figure 3: Schematic of a spray booth ventilation setup

During plant operation, the hot water mass flow rate and its supply and return temperatures are recorded, thus enabling to estimate the heat flow rate. Weather data (temperature and humidity) from a plant-side weather station is loaded into the model as boundary conditions.

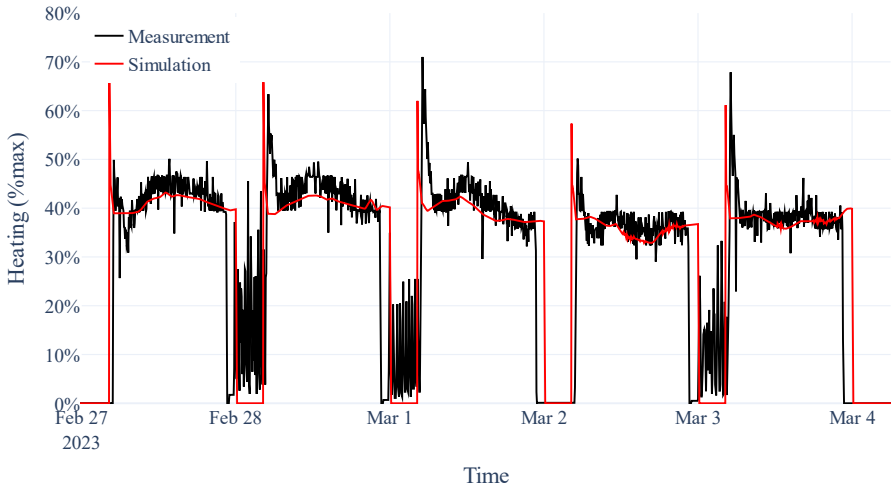

Figure 4: Measured and simulated heat flow rate of an air supply unit

The plant schematics and commissioning protocols provide information on most process variables, such as air mass flow rate, controller set-points, and HVAC component dimensioning. However, the effectiveness of sensible and latent heat transfer, which characterizes the performance of the thermal wheel, is not known beforehand.

Initially, constant values for effectiveness were assumed for the thermal wheels. However, during the calibration process, it became clear that this assumption was insufficient. The measurement data indicated higher effectiveness values at low inlet air temperatures. As a result, a temperature-dependent performance characteristic was implemented. The parameters of the characteristic were adjusted until the simulation results and measurement data showed good agreement.

Figure 4 shows the simulated and measured heating during a selected week. During regular operation, a good agreement between simulation and measurement is observable.

Drying ovens

This section presents the calibration of the drying oven for the e-coating process. The oven uses the exhaust gas from the DFTO air cleaning process. The DFTO unit employs an internal heat exchanger that transfers heat from the combustion chamber outlet to the DFTO inlet. Geometric data of the oven zones, volume flow rates of the fans and the gas heater capacity were obtained from schematics and commissioning protocols. The available measurement data includes time series of gas demand and snapshots of measured temperatures, preferably taken when the process is running at nominal load. Additionally, temperature curves of the car bodies are available, so the heat absorption by cars is known.

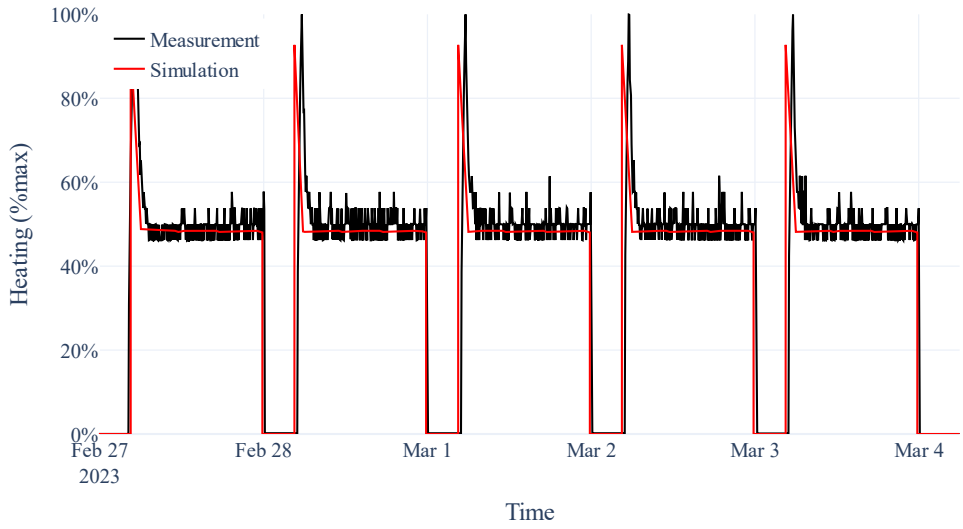

Figure 5: Measured and simulated heat flow rate of a e-coat drying oven

The temperatures of the exhaust gas were used to calibrate the oven zones' heat losses via convection and conduction. The internal heat exchanger's effectiveness was determined using transient measurement data of the gas demand. The resulting simulation results were compared to the measurement data in Figure 5, demonstrating good agreement.

RESULTS

Depending on the intended scope of research, the calibrated models can be connected to larger models, up to a model that simulates the entire paintshop. A whole-year simulation of the entire plant, and three analyses of plant optimization concepts are presented in the following sections.

Analysis of annual energy demand

This section presents a whole-year simulation of a paintshop model.

Model and simulation setup. For this analysis, the model of the entire paintshop is required. Due to the large number of modelled processes, the original model is large and contains more than 120000 equations. Weather data is obtained from EnergyPlus [12] for a typical weather profile based on weather data in Berlin, Germany. The production schedule is depicted in Figure 6 an follows a two-shift pattern: Production starts at 6:00 and ends at 22:00 (two 8-hour shifts) from Monday to Friday. The plant start-up and shutdown procedures are shown in Figure 7: Ventilation is turned on 1.75 hours before production to flush the plant of any unwanted substances. Heating is initiated 1.5 hours before production to allow sufficient time for the plant's heat capacities to warm up. It is assumed that production is always at full capacity and that the plant experiences no downtimes beyond the regular schedule, such as holidays or extended maintenance breaks.

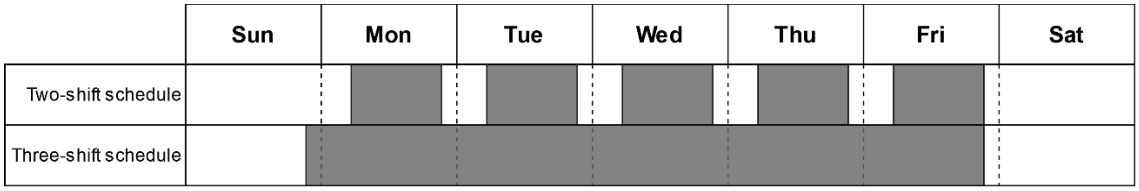

Figure 6: Weekly production schedules

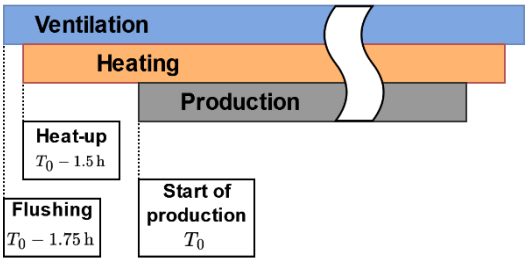

Figure 7: Start-up and shutdown sequence

The plant model including the production schedule, weather data and process models is then compiled and exported to a co-simulation Functional Mock-up Unit (FMU) that can be executed by other tools. DASSL is used as the numerical integrator. A Python simulator loads the FMU using the FMPy library, divides the simulation time of 1 year into smaller sections and distributes the tasks into separate processes to speed up computation. Once all simulations have terminated, the results are merged for further post-processing.

Heating and cooling demand: Profiles and annual consumption. The simulation yields the heat and mass flows of all modeled processes. Figure 8 shows the heating demand profile of the paintshop categorized into hot water and gas heating. The drying ovens are mostly gas-fired and, as shown in Figure 5, not depending on weather conditions. Hot water is mainly used as a heat source by HVAC units, which are highly dependent on weather conditions. This is reflected in the results, which indicate that the heating demand at cold temperatures is around twice as high as in summer. The load peaks that occur when the system starts are also clearly visible in the heating profile.

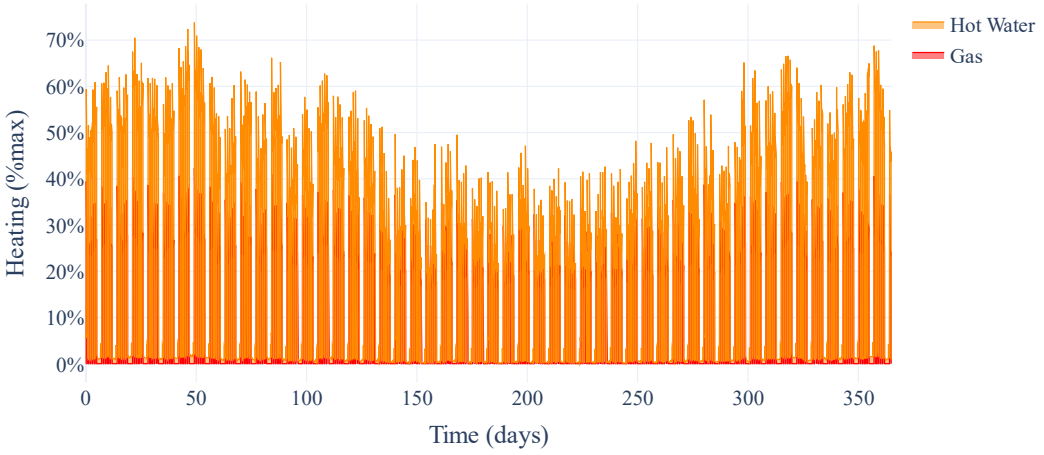

Figure 8: Simulated heating demand profile of a paintshop over a typical year

Figure 9 shows the annual consumption resulting from the numerical integration of gas heating, hot water heating, and cooling. The diagram reveals that the heating demand is significantly higher than the cooling demand. A considerable portion of the heating demand is already met through hot water, making it easy to decarbonize. However, the majority of heating is provided by burning gas, which requires more effort to electrify.

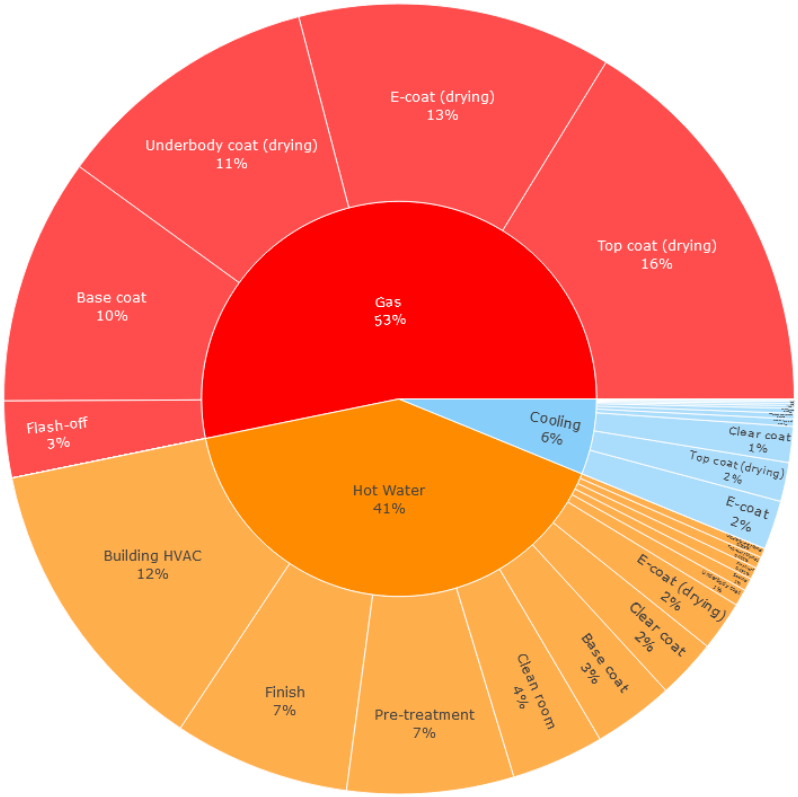

Figure 9: Annual energy consumption by source and process

Analysis of energy-saving measures

Since there is a good agreement between the simulated and measured data after model calibration, the model is considered accurate enough to assess plant modifications aimed at reducing energy consumption. The following sections present a selection of energy-saving measures and evaluate the potential energy savings if they are implemented.

Three-shift schedule. As evident from the presented data and results, peak loads occur at plant start-up. By increasing the operating time to three 8-hour shifts per day, the amount of start-up procedures is reduced from five start-ups to one start-up per working week. To evaluate the annual savings, the model of the entire plant is used and simulated twice with the same weather data, but different production schedules depicted in Figure 6.

Table 1: Simulated annual energy consumption of a paintshop operated with different production schedules

	Two-Shift Schedule	Three-Shift Schedule	Δ
Operating times (hours)			
Ventilation	4810	6344	+31.89%
Heating	4680	6318	+35.00%
Production	3900	5824	+49.33%
Energy demand			
Heating+Cooling $Q_{total,2s}$	100% ($Q_{total,2s}$)	133.86%	+33.86%
Heating (gas)	53.21% of $Q_{total,2s}$	70.85% of $Q_{total,2s}$	+33.14%
Heating (hot water)	40.60% of $Q_{total,2s}$	55.41% of $Q_{total,2s}$	+36.46%
Cooling	6.19% of $Q_{total,2s}$	7.60% of $Q_{total,2s}$	+23.04%

The simulation results are summarized in Table 1. The addition of an extra shift increases the production time, resulting in an increase of approximately 50% in the number of cars produced. Ventilation and heating times increase less, as there are less start-up and shutdown procedures. The results also indicate that the hot water heating, gas heating and cooling demands increase by 33.86% in total and thus by a lower extent compared to production time. When comparing the energy demand per vehicle produced, switching to the three-shift schedule leads to a reduction of around 10.4%.
Additionally, cooling demand increases less than heating demand. This can be explained by the weather conditions during the additional shifts. The new shifts are scheduled at night when temperatures are generally lower, resulting in higher heating demand and lower cooling demand compared to day shifts.

Vapor-compression heat pump for simultaneous heating and cooling. This section presents the analysis of a heat pump concept for supplying heating and cooling for the pre-treatment and e-coating processes. These processes are successive production steps and therefore usually in close proximity to each other. When the plant is running in nominal operation, the processes require nearly constant heating (pre-treatment) and cooling (e-coat), making it a suitable use case for heat pump integration.

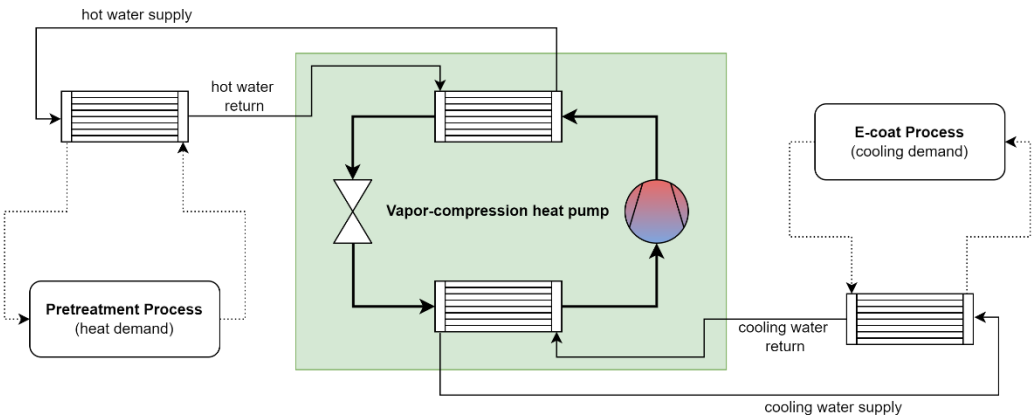

Figure 10: Heat pump integration into pre-treatment and e-coat processes

Figure 11Figure 10 shows how a heat pump can be integrated into the process: The returning cooling water (12 °C) from the e-coat process is fed into the evaporator, where it transfers heat to the heat pump refrigerant, thereby cooling down to the target supply temperature (6 °C). The evaporated refrigerant is then compressed to a target pressure at which the required condensation temperature is reached. In the condenser, hot vapor transfers heat to the hot water cycle before the flow is throttled to low pressure. The hot water is used to supply heat to the pre-treatment process.

The heat pump is designed to meet the entire cooling demand and a part of the heating demand. The performance is assessed with the Carnot efficiency heat pump model from the Buildings library, where the coefficient of performance (COP) is calculated using an assumed Carnot efficiency (ratio of achieved COP to Carnot COP) of 50%, which in line with reported values of available heat pumps [13]. Currently, the temperatures of the hot water cycle (130 °C supply, 80 °C return) is much higher than the temperature requirements of the pre-treatment process (up to 60 °C). To improve heat pump efficiencies, the hot water temperatures can be lowered.

Table 2: Performance of a chiller/heat pump for simultaneous cooling and heating in e-coating and pre-treatment

	Current configuration	**Configurations with lowered hot water temperatures**	
Hot water return/supply temp.	**80 → 130 °C**	**60 → 90 °C**	**65 → 75 °C**
Cooling $\dot{Q}_c$, normalized (12 → 6 °C)	100 %		
Heating to cooling $\dot{Q}_h/\dot{Q}_c$	184.93 %	154.79 %	148.63 %
Electric power to cooling $P_{el}/\dot{Q}_c$	85.21 %	54.79 %	48.49 %
Condensation temperature	135 °C	93 °C	78 °C
Evaporation temperature	4 °C	4 °C	4 °C
COP (chiller)	**1.17**	**1.83**	**2.06**
COP (heat pump)	**2.17**	**2.83**	**3.06**
COP, combined	**3.34**	**4.66**	**5.12**

Table 2 summarizes the results of the heat pump performance analysis for the current and lowered hot water temperatures. As per the Carnot cycle efficiency, the chiller/heat pump performs better when the sink temperature (hot water) is lower, albeit at a lower heating capacity. The best hot water temperature configuration (75 °C supply, 65 °C return) results in a cooling COP of 2.06 and a heating COP of 3.06, yielding a combined COP of 5.12. These are good prerequisites for a cost-effective retrofit measure. Further increase of COP is expected when the cooling water temperature is increased to values closer to the e-coat tank temperatures. However, economic feasibility requires further assessment, including the cost of electrical energy and gas. The required condensation temperature of 78 °C falls well within the range of available heat pumps and refrigerants.

Optimal control of paint booth air supply. This analysis examines the potential energy savings that can be achieved by modifying the controller of an air supply unit. Figure 3 illustrates the ventilation concept of a spray booth. To maintain optimal conditions inside the spray booth, the temperature must be kept between 22 and 24 °C, and the relative humidity between 40 and 70%. Typically, controllers are set to a fixed set-point in the center of the allowed ranges, such as 23 °C and 55% rH. A simulation was conducted to evaluate the potential savings that could be achieved by utilizing the entire allowed range.

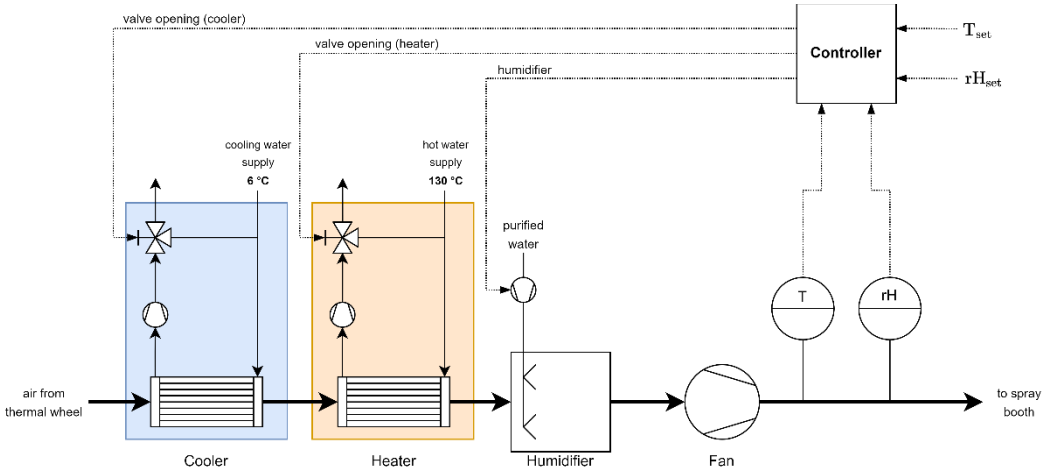

Figure 11: Schematic of an air supply unit with temperature and humidity control

Figure 11 shows the structure of the air supply unit for controlling temperature and humidity. Air from the thermal wheel is drawn into the unit, where it flows through the cooler. The cooler fulfills two purposes: By cooling the air with cooling water, the temperature will drop, and the humidity also decreases due to condensation of water. The heater increases the air temperature via the hot water cycle. The humidifier increases the humidity in an isenthalpic change of state using spray humidification. Air is moved by the fan at the air supply unit's outlet and adds work to the air depending on pressure increase and isentropic efficiency. Temperature and relative humidity are measured at the outlet and act as controlled variables for the HVAC controller.

Both control schemes were implemented and simulated using the same weather data and a three-shift schedule for one year. Table 3 summarizes the results and compares the analyzed control schemes. Using the entire allowable range leads to large savings of heating and cooling.

Table 3: Energy demand for air supply units with different control schemes

	Fixed set-point controller	Optimized controller	Δ
Temperature set-point	23 °C	22 to 24 °C	-
Relative humidity set-point	55 %	40 to 70 %	-
Heating + Cooling $Q_{total,AS}$	100% ($Q_{total,AS}$)	53.48% of $Q_{total,AS}$	-46.53%
Heating demand	35.96% of $Q_{total,AS}$	14.13% of $Q_{total,AS}$	-60.7%
Cooling demand	64.04% of $Q_{total,AS}$	39.35% of $Q_{total,AS}$	-38.6%

To illustrate how the savings are achieved, Figure 12 shows the trajectory of the air conditioning for a selected point in time with about 10 °C outside temperature at 38% rH. After the air has passed through the thermal wheel, the air already has a sufficiently high humidity ratio. As a result, the optimized controller does not humidify and adds only enough heat to reach the minimum target temperature, while the fixed set-point controller must overheat to compensate for the cooling by humidification. Similar improvements in control behavior are found for all weather conditions, resulting in the savings shown in Table 3.

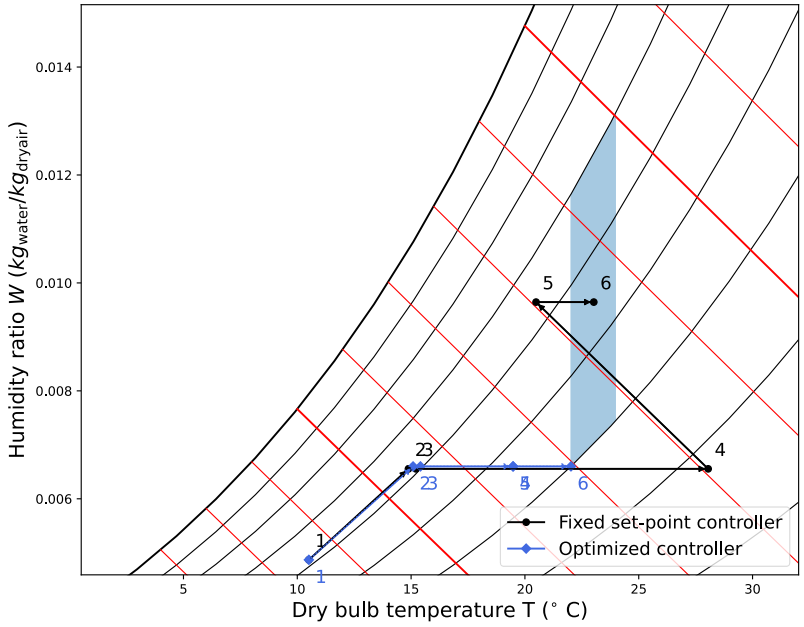

Figure 12: Trajectory of the air conditioning for cold outside conditions in a psychrometric chart. Blue area indicates the allowable air conditions. Indices: (1) outside, (2) after thermal wheel, (3) after cooler, (4) after heater, (5) after humidifier, (6) outlet

CONCLUSION

This study presents a methodology for assessing and improving energy efficiency of automotive paintshops. Through implementation of dynamic models using Modelica and calibration with transient data from operating paintshops, the study successfully demonstrates how dynamic simulation can be employed to the efficacy of various energy-saving measures. These measures, ranging from adjustments in production schedules to the integration of heat pump systems and optimization of HVAC control, demonstrate significant potential for reducing energy consumption: Switching to a three-shift schedule reduces energy demand per vehicle produced by 10.4%. A heat pump can be operated at a combined (heating and cooling) COP of 5.12 when integrated into the pre-treatment and e-coat processes. Optimizing the controller of an air supply unit reduces its annual energy demand by 46.5%.

NOMENCLATURE

Abbreviations	
COP	Coefficient of performance
DASSL	Differential algebraic system solver
DFTO	Direct-fired thermal oxidizer
FMU	Functional Mock-up Unit
HVAC	Heating, ventilation and air conditioning
rH	Relative humidity
RTO	Regenerative thermal oxidizer
VOC	Volatile organic compounds
Symbols	
P_{el}	Electric power
Q	Heat, energy
$\dot{Q}$	Heat flow rate (heating or cooling)
T	(Dry bulb) Temperature
W	Humidity ratio
Subscripts	
2s	Two-shift
AS	Air supply
C	Cooling
El	Electric
H	Heating

REFERENCES

[1] BMW Group, "Sustainability & Responsibility: CO2 Reduction.," https://www.bmwgroup.com/en/sustainability/co2-reduction.html, [retrieved 27 March 2024].

[2] Volkswagen AG, "Group Sustainability Report 2022," 2023, https://www.volkswagen-group.com/en/publications/more/group-sustainability-report-2022-1644.

[3] Giampieri, A., Ling-Chin, J., Ma, Z., Smallbone, A., and Roskilly, A. P., "A review of the current automotive manufacturing practice from an energy perspective," *Applied Energy*; Vol. 261, 2020, p. 114074. doi: 10.1016/j.apenergy.2019.114074.

[4] Giampieri, A., Ma, Z., Ling-Chin, J., Smallbone, A. J., and Roskilly, A. P., "A techno-economic evaluation of low-grade excess heat recovery and liquid desiccant-based temperature and humidity control in automotive paint shops," *Energy Conversion and Management*; Vol. 261, 2022, p. 115654. doi: 10.1016/j.enconman.2022.115654.

[5] Alt, S., and Sawodny, O., "Model-based temperature and humidity control of paint booth HVAC systems," *2015 IEEE International Conference on Mechatronics (ICM)*, IEEE, 2015, pp. 160–165.

[6] Wendt, J., Weyand, A., Barmbold, B., and Weigold, M., "Approach for Design of Low Carbon Footprint Paint Shops in the Automotive Industry," *Manufacturing Driving Circular Economy*, edited by H. Kohl, et al., Springer International Publishing, Cham, 2023, pp. 490–498.

[7] Johnson, T., Mark, A., Sandgren, N., Erhardsson, L., Sandgren, S., and Edelvik, F., "Efficient Simulation of Convective Ovens in Automotive Paintshops," *Journal of Heat Transfer*; Vol. 144, No. 9, 2022. doi: 10.1115/1.4054599.

[8] Daniarta, S., Kolasiński, P., and Rogosz, B., "Waste Heat Recovery in Automotive Paint Shop via Organic Rankine Cycle and Thermal Energy Storage System—Selected Thermodynamic Issues," *Energies*; Vol. 15, No. 6, 2022, p. 2239. doi: 10.3390/en15062239.
[9] Giampieri, A., *Low-grade Heat Recovery for Sustainable Automotive Manufacturing*, 2021.
[10] Wetter, M., Zuo, W., Nouidui, T. S., and Pang, X., "Modelica Buildings library," *Journal of Building Performance Simulation*; Vol. 7, No. 4, 2014, pp. 253–270. doi: 10.1080/19401493.2013.765506.
[11] Streitberger, H.-J., ed., *Automotive paints and coatings*, 2nd edn., Wiley-VCH-Verl., Weinheim, 2008.
[12] National Renewable Energy Laboratory, "EnergyPlus: Weather Data," https://energyplus.net/weather, [retrieved 27 March 2024].
[13] Arpagaus, C., Bless, F., Uhlmann, M., Schiffmann, J., and Bertsch, S. S., "High temperature heat pumps: Market overview, state of the art, research status, refrigerants, and application potentials," *Energy*; Vol. 152, 2018, pp. 985–1010. doi: 10.1016/j.energy.2018.03.166.